Heliyon 9 (2023) e20201

Contents lists available at ScienceDirect

Heliyon

journal homepage: www.cell.com/heliyon

Engineered elastin-like polypeptide improves the efficiency of adipose-derived stem cell-mediated cutaneous wound healing in type II diabetes mellitus

Seung-Hwa Woo [a], Joon Hyuk Choi [b], Yun Jeong Mo [c], Yun-Il Lee [c], Won Bae Jeon [b,**], Young-Sam Lee [a,c,*]

[a] Department of New Biology, DGIST, Daegu, 42988, Republic of Korea
[b] Division of Biotechnology, DGIST, Daegu, 42988, Republic of Korea
[c] Well Aging Research Center, Division of Biotechnology, DGIST, Daegu, 42988, Republic of Korea

ARTICLE INFO

Keywords:
Engineered elastin-like polypeptide
Wound healing
Type II diabetes mellitus
Adipose-derived stem cells
Skin elasticity

ABSTRACT

Impaired cutaneous wound healing is a major complication in patients with diabetes mellitus (DM), leading to increased amputation and mortality rates in affected patients. Adipose-derived stem cells (ASCs) are widely used seed cells for promoted tissue regeneration to improve wound closure under diabetic conditions. However, ASCs-based therapies remain limited due to difficulties in maintaining cell quality during transplantation. To overcome this problem, extracellular matrix mimetic biomaterials have been developed for use in biomedical engineering field, including tissue engineering and regenerative medicine. Herein, a biosynthesized arginine–glycine–aspartate amino acid residues (RGD motif, known as a cell adhesion motif)-containing elastin-like polypeptides (REPs) improved the efficacy of ASCs in enhancing wound closure and skin elasticity in diabetic wounds by promoting the expression of angiogenic growth factors. Therefore, REPs can be used as potential supplements to stem cell-based therapeutic approach to accelerate diabetic wound repair.

1. Introduction

Diabetes mellitus (DM) is a chronic metabolic disorder that causes high blood sugar levels. DM is associated with chronic inflammation, circulatory dysfunction, neuropathy, impaired neuropeptide signaling, and cutaneous alterations [1,2]. Although the specific correlations between morphological changes in skin tissue and biological properties of DM remain unclear, DM is thought to cause thickening and diminished elasticity of the skin [3]. Skin elasticity is an indicator of skin function and health and improves the ability of the dermis to regenerate and remodel, which are important for effective wound repair [4]. Therefore, skin stiffening not only delays the wound healing process but also reduces the sensation of systemic pain, leading to chronic wounds in patients with DM [5,6]. Stem cell-based therapies, growth factor gene delivery, and angiotensin receptor analogs are currently used as wound healing treatments for DM [7]. However, diabetic wounds are still challenging to heal, so new methods are needed to effectively improve wound closure and subsequent skin elasticity recovery in patients with DM.

* Corresponding author. Department of New Biology, DGIST, Daegu, 42988, Republic of Korea.
** Corresponding author.
E-mail addresses: wbjeon@dgist.ac.kr (W.B. Jeon), lee.youngsam@dgist.ac.kr (Y.-S. Lee).

https://doi.org/10.1016/j.heliyon.2023.e20201
Received 9 May 2023; Received in revised form 12 September 2023; Accepted 13 September 2023
Available online 15 September 2023

Adipose-derived stem cells (ASCs), which are mesenchymal stromal cells, have beneficial properties, including a high yield, easy accessibility, and strong ability to modulate the immune system [8,9–12]. ASCs improve healing processes, healing rate, and scar repair by enhancing epithelia migration and angiogenesis [10–12]. Therefore, ASCs have been considered potential treatments for promoting the healing of chronic wounds in DM models. In addition, many therapeutic strategies include the combination of ASCs and biomaterials [13–15]. However, methods for maintaining the quality of ASCs during transplantation are still under investigation.

Elastin-like polypeptides (ELPs) are biopolymers that are derived from human elastin. ELPs are composed of repeated pentapeptides $(Val–Pro–Gly–X–Gly)_n$, where "X" denotes a variable residue that affects the general properties of ELPs, including the inverse transition temperature (T_t) at which ELPs undergo a reversible sol-gel shift [16]. Such a temperature-dependent phase transition is useful for applications involving responses to stimuli in biological environments. The structures and functions of ELPs can be controlled via genetic engineering to synthesize recombinant polypeptides. Moreover, ELPs can be used as carriers to deliver biological therapeutic agents to different anatomical sites for treating various diseases, such as cancer, type II DM, and osteoarthritis [17]. We previously biosynthesized arginine-glycine-aspartic acid (RGD)-containing elastin-like polypeptides (REPs), which are characterized by a $TGPG[VGRGD(VGVPG)_6]_{20}WPC$ structure, mimicking fibronectin–integrin interactions in the extracellular matrix (ECM), which contains a high density of integrin-binding ligands [18]. In a manner similar to fibronectin, REPs regulate various cellular behavior, including cell migration, adhesion, proliferation, and differentiation, thus showing great potential for improving the effects of stem cell-based therapeutic approach in tissue regeneration and remodeling. In particular, the REP matrix improves the efficiency of ASCs-mediated cutaneous wound healing by enhancing the viability of engrafted ASCs [19]. However, further studies on the specific functions of REPs in chronic wound healing, as well as the underlying mechanisms, are necessary.

In this study, we investigated whether REP supplement can improve the efficiency of ASCs-mediated tissue repair in an animal model of type II DM. We found that the administration of REPs aggregated to wounds to facilitate wound closure and enhanced angiogenesis in mouse model of DM. Furthermore, REP–ASC combination treatment improved skin elasticity. Therefore, REPs can be used to enhance the stem cell-based therapeutic potential and improve skin health during and after wound healing in patients with DM.

2. Materials and methods

2.1. REP preparation

The expression and purification of REPs as well as the determination of the T_t were performed as previously reported [18]. For experiments involving different concentrations of REPs, the REPs were serially diluted in Dulbecco's PBS.

2.2. Culture and maintenance of ASCs

ASCs isolated from inguinal white fat tissue in C57BL/6 mice (10MU-006; iXCells, San Diego, CA 92121, USA) were maintained in DMEM with low-glucose (LM001-11; WELGENE, Daegu, Korea) supplemented with 10% FBS and 1 × antibiotic-antimycotic solution (WELGENE). The cells were cultured under 5% CO_2 and low oxygen concentration (3% O_2) at 37 °C, passaged at a 1:3 dilution, and used before passage 3. A total of 70 000 cells were diluted in 25 μL of PBS for transplantation into wounds.

2.3. In vivo evaluation of the wound healing activity

One week before the wound-healing assay, blood glucose levels were measured using an Accu-Chek device (0123; Roche, Germany). Optimal fasting glucose levels were determined using a previously reported method [20]. The wound-healing assay were carried out with C57BL/6 (8 weeks old) and db/db (8–12 weeks old) male mice. All the experiments were approved by and followed the ethical guidelines of the Laboratory Animal Research Center of DGIST (approval no. DGIST-IACUC-21072201-0005). Splinted excisional wound model which mimics the biological human wound healing processes was applied to monitor the kinetics of skin repair [19,21,22]. In detail, to anesthetize the animal using the SomnoSuite Anesthesia System (Kent Scientific Corporation, Tokyo, Japan), mice were exposed to 1–1.5% isoflurane (Isotroy 100; Troikaa Pharmaceutical Ltd., Ahmedabad, India) in oxygen at 1 L/min of flow rate. Then, depilation of dorsal hair was performed using a shaver and depilatory cream. After skin disinfection with alcohol and povidone–iodine, full-thickness excisional wounds of 4- or 6-mm in diameter were created using a punch biopsy device (Kai Medical, Seki City, Japan), as needed for the experiment. Then, ring-shaped silicone splints (10 mm of inner/15 mm of outer diameter) were affixed using tissue adhesives (VetBond Tissue Adhesive, 3 M, Minneapolis, MN, US) around the wounds. The treatment was carried out referring to a previously published procedure [19]. Briefly, the 25 μL of phosphate-buffered saline (PBS), REP (50–150 μM), ASC (7×10^4 cells), or RA (100 μM REP combined with 7×10^4 ASC) were treated onto the wound and allowed to penetrate the skin for 5 min. Then, the wounds were protected with a clear, adhesive film (Tegaderm Film, 3 M). The treated mice were individually housed in cages. At different time points (up to day 21), the wound area was measured, and samples were collected for histological and gene expression analyses.

2.4. Immunohistochemistry (IHC)

A piece of skin wound samples cut in half were fixed with formalin (HT501128; Sigma–Aldrich, St. Louis, MO, USA) and embedded in paraffin. For histological analysis, approximately 4-μm thickness of paraffin sections were used. Hematoxylin and eosin (H&E), Masson's trichrome, and IHC staining for CD31 (ab28364 and ab182981; Abcam, Cambridge, MA, USA) was carried out at Bio-medical

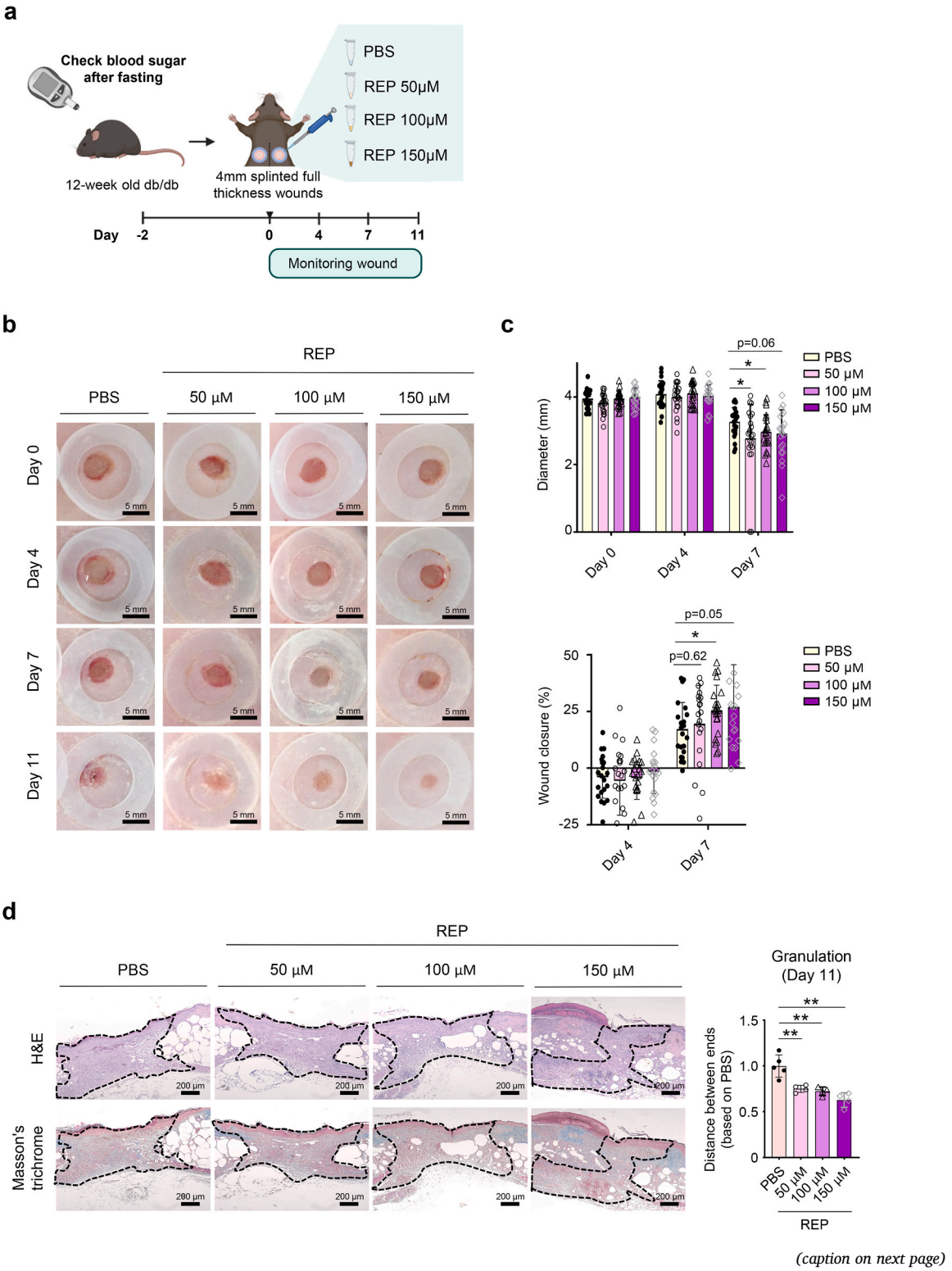

(caption on next page)

Fig. 1. REPs accelerate skin wound closure in db/db mice.
(a) Schematic of the experimental procedure. Twelve-week-old db/db mice were randomly divided into four groups after measuring their blood sugar levels. Two excisional wounds were generated in the dorsal skin with a 4-mm biopsy punch. The wounds in each group were treated with PBS or REPs (50, 100, and 150 μM). The wound healing process was monitored for 11 days. **(b)** Representative images of the wound healing process. Scale bar = 5 mm. **(c)** Changes in the average wound diameter and percent wound closure. Each data point corresponds to a single wound (the number of wound ≥20 in each group). **(d)** H&E staining (top) and Masson's trichrome staining (bottom) of the wound after day 11. Scale bar = 200 μm. The granulation tissue border is marked with a dashed line. Changes in the granulation size (right). Each data point corresponds to a single wound (the number of wound = 4–5 in each group). The data are presented as the mean ± SD. For statistical analyses in **(c–d)**: *$p < 0.05$ according to multiple *t*-test **(c)** and **$p < 0.01$ according to unpaired *t*-test **(d)** compared to the PBS group.

research institute in Kyungpook National University Hospital (Daegu, Korea) and at Histoire (Seoul, Korea). Stained slides of skin tissue were observed under a microscope (Stereo Investigator; Zeiss, Oberkochen, Germany).

2.5. Reverse transcription-quantitative polymerase chain reaction (RT-qPCR) analysis

The other piece of skin wound samples cut in half were frozen at −80 °C. Total RNA was purified using QIAzol lysis reagent (#79306; QIAGEN, Hilden, Germany) according to the manufacturer protocol. The Transcriptor First Strand cDNA Synthesis Kit (04 896 866 001; Roche, Germany) was used for cDNA synthesis after determining the RNA concentration using a spectrophotometer (NanoDrop One C, Thermo Fisher, UK) and the RNA integrity via electrophoresis. Quantitative PCR on Light Cycler 480 II detection system (Roche) was performed with the KAPA SYBR FAST qPCR Master Mix (2 ×) (07959397001; Sigma–Aldrich). The PCR cycle conditions were as follows: 5 min at 95 °C; 45 cycles of 10 s each at 95 °C, 60 °C, and then 72 °C. The relative amount of target mRNA in samples was estimated using the comparative cycle threshold (C_t) value and normalized to that of glyceraldehyde 3-phosphate dehydrogenase (Gapdh, control). The following primers were used to detect specific gene expression: S1pr1 forward (5′-GCGCTCAGAGACTTCGTCTT-3′), S1pr1 reverse (5′-AAACAGCAGCCTCGCTCAA-3′), Cd31 forward (5′-GCCTCACCAAGAGAACGGAA-3′), Cd31 reverse (5′-TAGCGCCTCTGAGTCTCTGT-3′), Vwf forward (5′-ATGAGAAGAGGCCTGGGGAT-3′), Vwf reverse (5′-TTCTGCCCATCGAAGGTGAC-3′), Nos3 forward (5′-GCTGCGGGATCAGCAACG-3′), Nos3 reverse (5′-GGGGAGGAAGACTGTCAGGA-3′), Mki67 forward (5′-CCAGCACTCCAAAGAAACCC-3′), Mki67 reverse (5′-ATTTTGTAGGGTCGGGCAGG-3′), Pik3r1 forward (5′-GGCTGGGGTGTGTGATGTAA-3′), Pik3r1 reverse (5′-GGGCAGTGCTGGTGGAT-3′) Gapdh forward (5′- AGGTCGGTGTGAACGGATTTG-3′), Gapdh reverse (5′- TGTAGACCATGTAGTTGAGGTCA-3′). Primers were purchased from Bioneer (Daejeon, South Korea).

2.6. Measurement of skin elasticity

The mice were anesthetized using isoflurane. Then, skin elasticity in the healed area was measured using a Skin Analyzer Imaging System (Courage + Khazaka Electronic MPA 580, Köln, Germany) following the manufacturer's protocol.

2.7. Statistical analyses

All the data were analyzed using GraphPad Prism version 7 (GraphPad Software, USA). *t* tests (as nonparametric tests) and multiple *t* tests (as grouped analysis) were used to conduct all the statistical analyses. In the Figure Legends, statistical analysis methods are specified. Differences were considered statistically significant at $p < 0.05$ for in vitro studies and $p < 0.1$ for in vivo studies.

3. Results

3.1. REPs accelerate skin wound closure in db/db mice by regulating angiogenic factor expression

REPs accelerate wound closure in nondiabetic mice by increasing keratinocyte migration and collagen matrix synthesis [19]. However, the material has not been tested in diabetic wound where the healing is retarded, causing an increased risk of infectious complications. Meanwhile, prior to determining the effects of REPs on the wound healing in diabetic condition, we first confirmed the experimental condition with the severity of impaired skin wound healing in a diabetic mice model. Diabetic wound repair and the effects of therapies have been extensively studied in various mouse models. Among these models, the db/db mouse, a type II DM animal model with a spontaneous mutation in the leptin receptor, exhibits severe impairments in wound repair [23]. Thereby, we compared the wound closure rate of splinted cutaneous wounds (6 mm diameter) in db/db mice with elevated glucose levels (blood glucose level ≥250 mg/dL) and nondiabetic C57BL/6J mice with normal glucose levels (blood glucose level ≤150 mg/dL) (Supplementary Fig. 1a). Indeed, wound closure was markedly retarded in db/db mice compared with nondiabetic mice. The average wound area significantly differed after day 7. Notably, complete wound closure required more than 21 days in db/db mice but only 14 days in nondiabetic mice (Supplementary Figs. 1b–c). These results indicate that db/db mice are suitable models for studying the therapeutic effects of biomaterials on the skin wound healing in diabetic condition. Of note, in the subsequent experiments, we reduced the wound size to 4 mm diameter to monitor the treatment's effect in diabetic wound healing within three weeks.

To determine whether REPs exert therapeutic effects on chronic diabetic wounds, various concentrations of REPs (0–150 μM) were administered to full-thickness splint wound sites (4 mm diameter) in the dorsal skin of db/db mice (Fig. 1a). Similar to a previous report in nondiabetic mice, in this study, REPs accelerated wound closure in db/db mice in a dose-dependent manner; in particular,

≥100 μM REP exerted therapeutic effects on day 7 (Fig. 1b and c). H&E staining revealed that the amount of granulation tissue was inversely correlated with the REP concentration on day 11. Moreover, Masson's trichrome staining presented that the collagen-positive area was increased in a REP concentration-dependent manner (Fig. 1d). Therefore, 100 μM REP, which had a degree of stickiness similar to that of phosphate-buffered saline (PBS), was selected for the subsequent experiments.

Next, we performed repeated wound healing experiments with REPs to determine the specific factors that are involved in REP-induced accelerated wound healing in db/db mice. We found that 100 μM REP significantly accelerated wound healing beginning on day 4 (Fig. 2a and b). In addition, the granulation tissue area continuously decreased in the REP group beginning on day 11 (Fig. 2c). Implanted REPs increase the expression levels of vascular endothelial growth factor (VEGF), CD31, and von Willebrand factor and promote angiogenesis in normal skin [19]. The db/db mice exhibit impaired angiogenesis due to dysfunctional receptors, reduced levels of key ligands or numbers of cells, and failure of epithelial-mesenchymal transition, so improving angiogenesis is a potential strategy for accelerating wound healing in db/db mice [24]. Here, compared to the PBS-treated group, the number of CD31-positive cells was increased in the REP-treated group on day 11 (Fig. 2d). Notably, the REP group exhibited a distribution of adipose tissue that was similar to that in normal skin. Moreover, the REP group exhibited significantly upregulated gene expression, involved in angiogenesis, including sphingosine-1-phosphate receptor 1 (*S1*pr*1*) and nitric oxide synthase 3 (*Nos3*) (Fig. 2e). Taken together, these

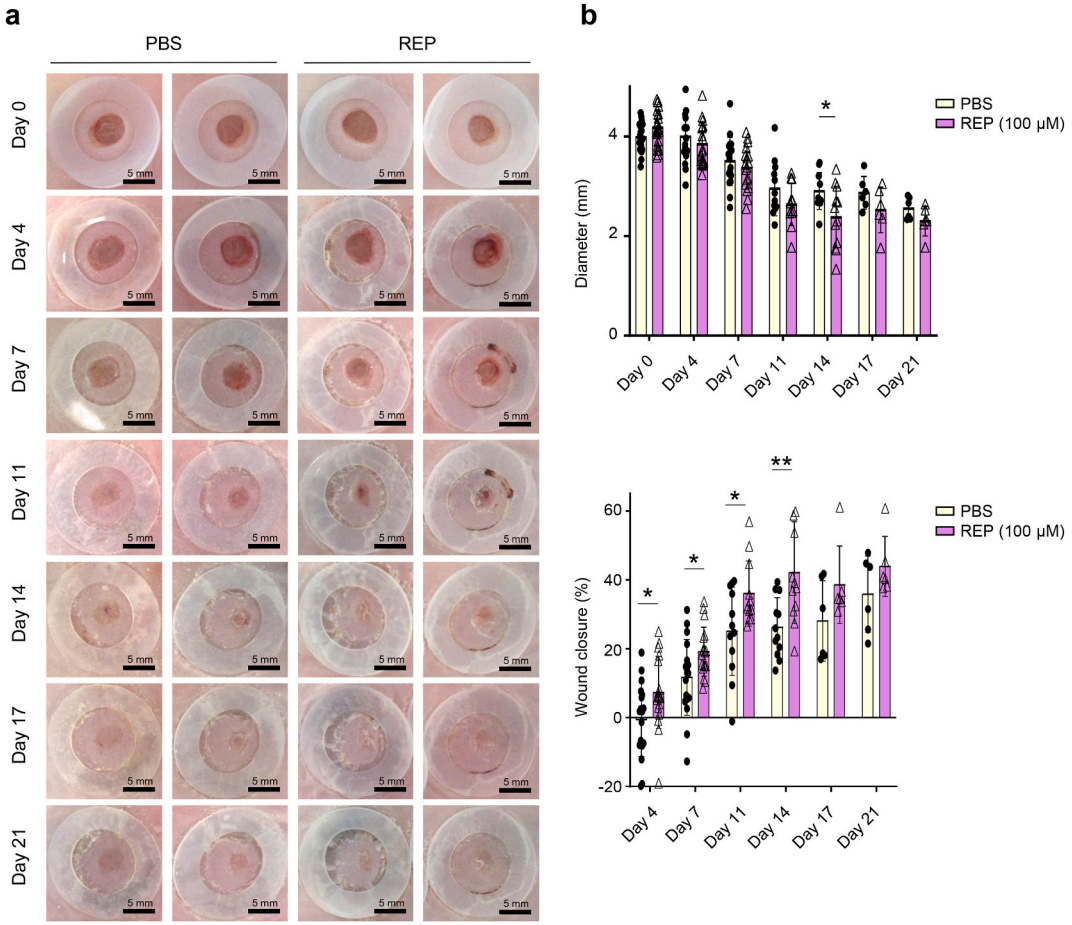

Fig. 2. REPs regulate angiogenic factor expression in db/db mice.
(a) Twelve-week-old db/db mice were randomly divided into two groups after measuring their blood glucose levels. Two excisional wounds were generated in the dorsal skin with a 4-mm biopsy punch. The wounds in each group were treated with PBS or 100 μM REP. The wound healing process was monitored for 21 days. Scale bar = 5 mm. **(b)** Changes in the average wound diameter and percent wound closure. Each data point corresponds to a single wound (the number of wound ≥6 in each group). **(c)** H&E staining (left) and Masson's trichrome staining (middle) of the skin at wound site during healing. Scale bar = 400 μm. The granulation tissue border is marked with a dashed line. Changes in the granulation size (right). Each point corresponds to a single wound (the number of wound = 3 in each group). **(d)** Immunostaining for CD31 in the control group and the REP group. Scale bar = 10 μm (higher magnification images) or 100 μm (lower magnification). The number of CD31-positive cells (in brown color) was measured with ImageJ software (IHC tool). The amount of stained cells in each view field is represented by each data point (n = 11–12). **(e)** mRNA expression of wound healing markers, including genes that are associated with angiogenesis, proliferation, and differentiation. The data shown are mean ± SD. n = 3 (biological replicate). For statistical analyses in **(b–e)**: *p < 0.05, **p < 0.01 according to multiple *t*-test **(b, e)** and **p < 0.01, ****p < 0.0001 according to unpaired *t*-test **(c)** compared to the PBS group.

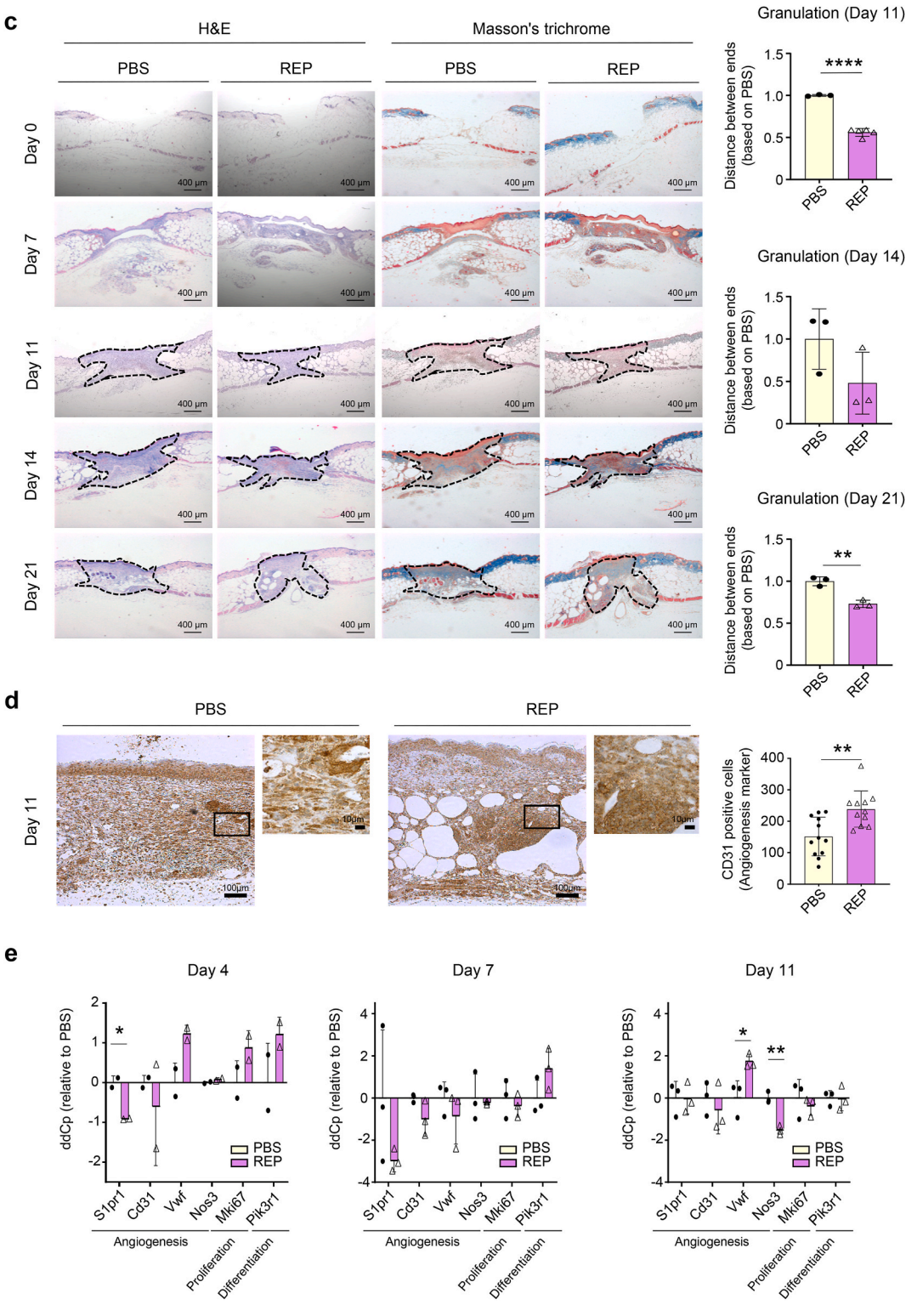

Fig. 2. (*continued*).

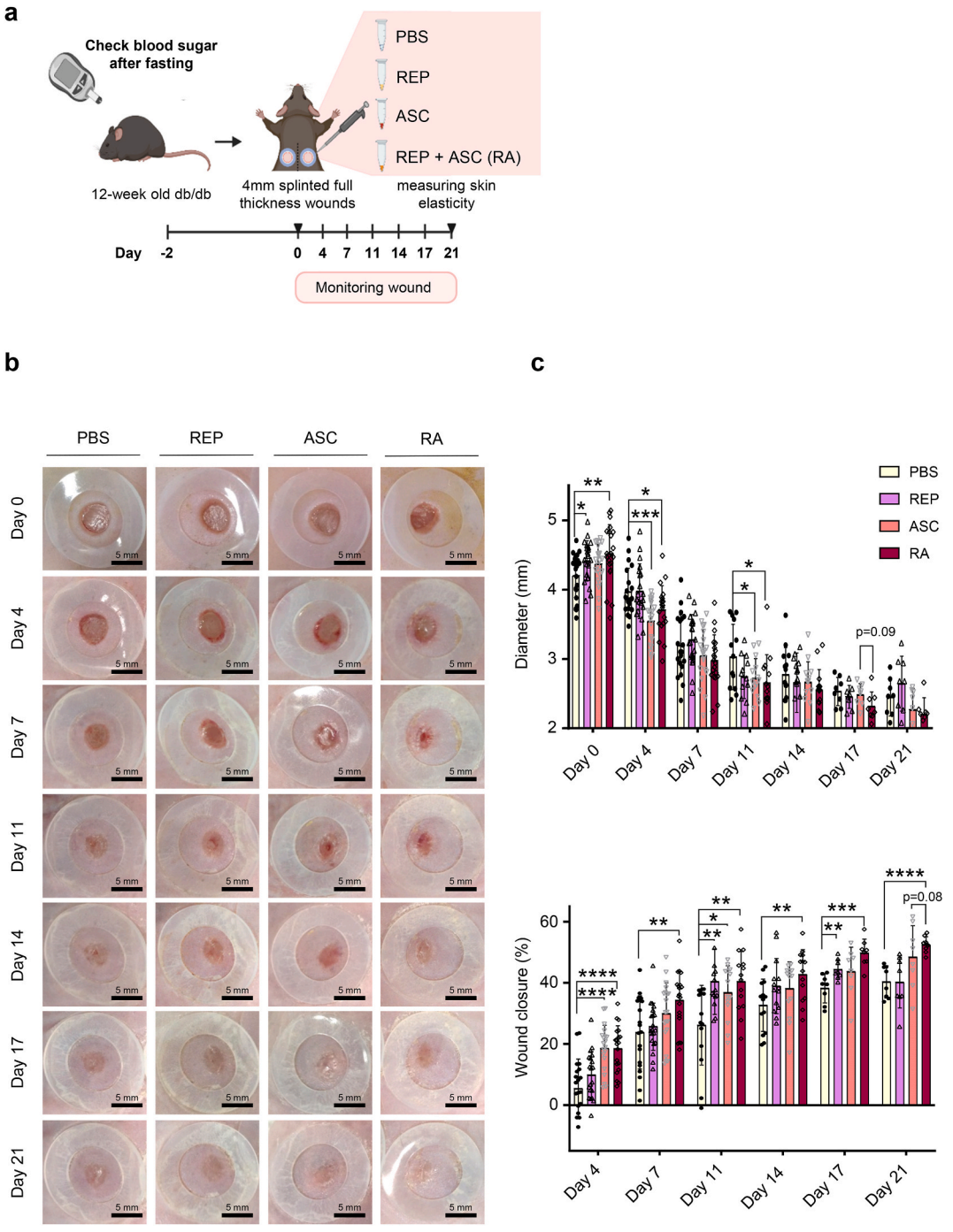

Fig. 3. REPs improve the efficiency of adipose-derived stem cell-mediated wound healing with increasing skin elasticity.
(a) Schematic of the experimental procedure. Ten-week-old db/db mice were randomly selected into four groups after measuring their blood glucose levels. Two full-thickness wounds were generated in the dorsal skin of mice with a 4-mm biopsy punch. The wounds in each group were treated with PBS (control group), 100 μM REPs (REP group), ASCs (ACS group), or 100 μM REP + ASC (RA group). The wound healing process was monitored for 21 days. **(b)** Representative images of the wound healing process. Scale bar = 5 mm. **(c)** Changes in the average wound diameter and percent wound closure. Each point corresponds to a single wound (the number of wound ≥8 in each group). **(d)** Representative images of H&E and Masson's trichrome staining of the wound during healing (left). Scale bar = 200 μm. The granulation tissue border is marked with a dashed line. Changes in the granulation size (right). Each point corresponds to a single wound (the number of wound = 2–6 in each group). **(e)** Immunostaining for CD31 in the control, REP, ASC, and RA group. Scale bar = 10 μm (higher magnification) or 100 μm (lower magnification). **(f)** Quantification of CD31-positive cells in each group. The amount of positively stained cells in each view field is represented by each data point (n = 25–30). **(g)** Skin elasticity level on day 21 after wounding. Each point corresponds to a single wound (the number of wound = 16 in each group). The data shown are

mean ± SD. For statistical analyses in **(c–g)**: *p < 0.05, **p < 0.01, ***p < 0.001, and ****p < 0.0001 according to multiple *t*-test **(c)** and according to unpaired *t*-test **(d–g)**.

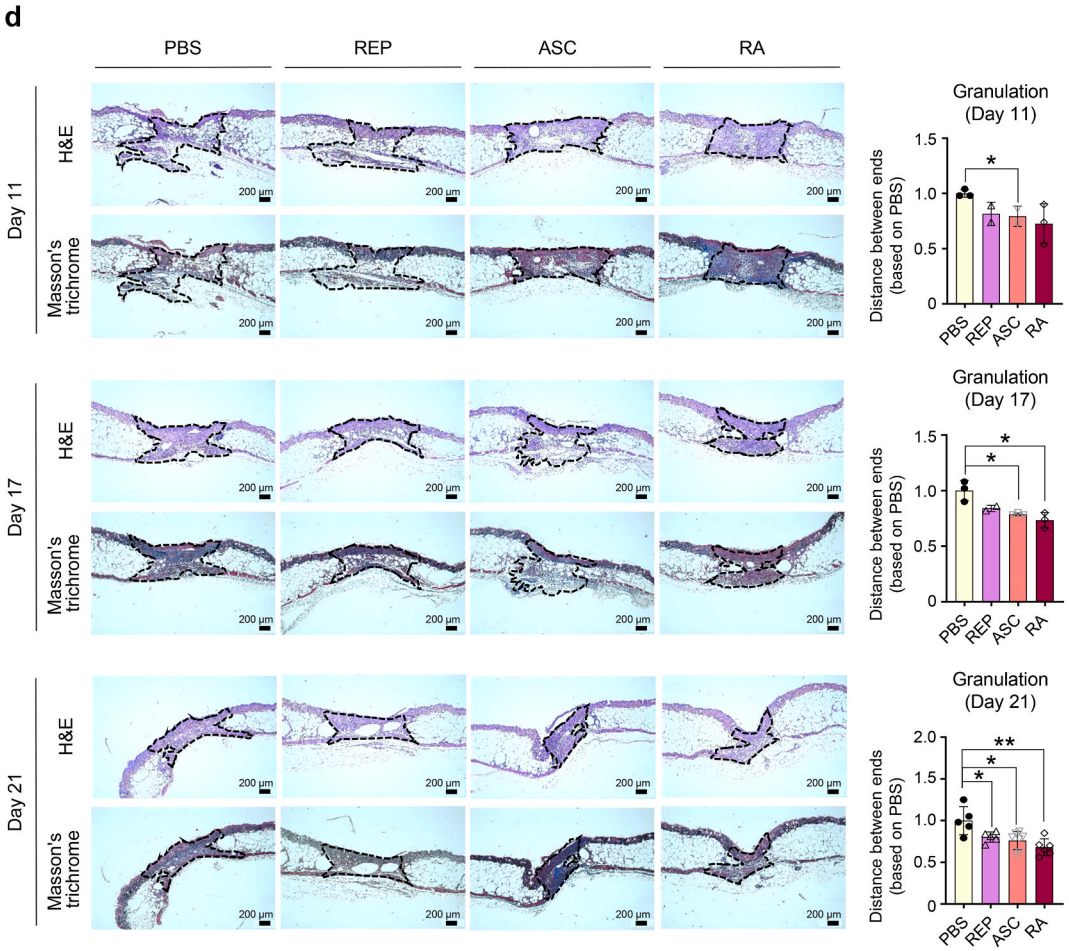

Fig. 3. (*continued*).

results indicate that REPs accelerate the healing of skin wounds by improving angiogenesis in db/db mice.

3.2. REPs enhance the functions of ASCs and skin elasticity to promote effective wound healing

ASCs improve angiogenesis and wound healing and inhibit abnormal scar formation [10–12]. REPs improve the survival of ASCs that are transplanted into normal mouse skin wounds and enhance their wound healing effects [19]. However, the specific effects of REP on scar formation and fibrosis after wound healing remain unknown. Therefore, we determined whether REPs enhanced the beneficial effects of ASCs on skin wound repair in the diabetic mice (Fig. 3a). Wound closure was significantly accelerated in the REP-ASC combination (RA) group compared with the PBS group and slightly enhanced compared with the ASC group (Fig. 3b and c). Additionally, the granulation tissue area on day 21 was significantly reduced in either the REPs- or ASCs-containing group (REP, ASC, and RA group), compared with the PBS group (Fig. 3d). Consistent with the results in Fig. 2d, the number of CD31-positive cells was significantly increased in the REPs-containing group compared to the PBS group, and the number was further enhanced in the RA group on day 21 (Fig. 3e and f). ASCs inhibit scar formation in diabetic wounds [25]. Skin elasticity affects skin stiffness, wound healing, scar formation, and fibrosis (keloids) [5,26]. Therefore, we examined the effects of REPs on skin elasticity after wound healing in db/db mice. Interestingly, the elasticity of the recovered skin was significantly increased in the RA group on day 21 (Fig. 3g). These results indicate that REPs enhance the functions of ASCs in the overall wound healing and remodeling process under diabetic conditions.

4. Discussion

Type II diabetes is a global health problem that is associated with serious complications, including impaired wound healing,

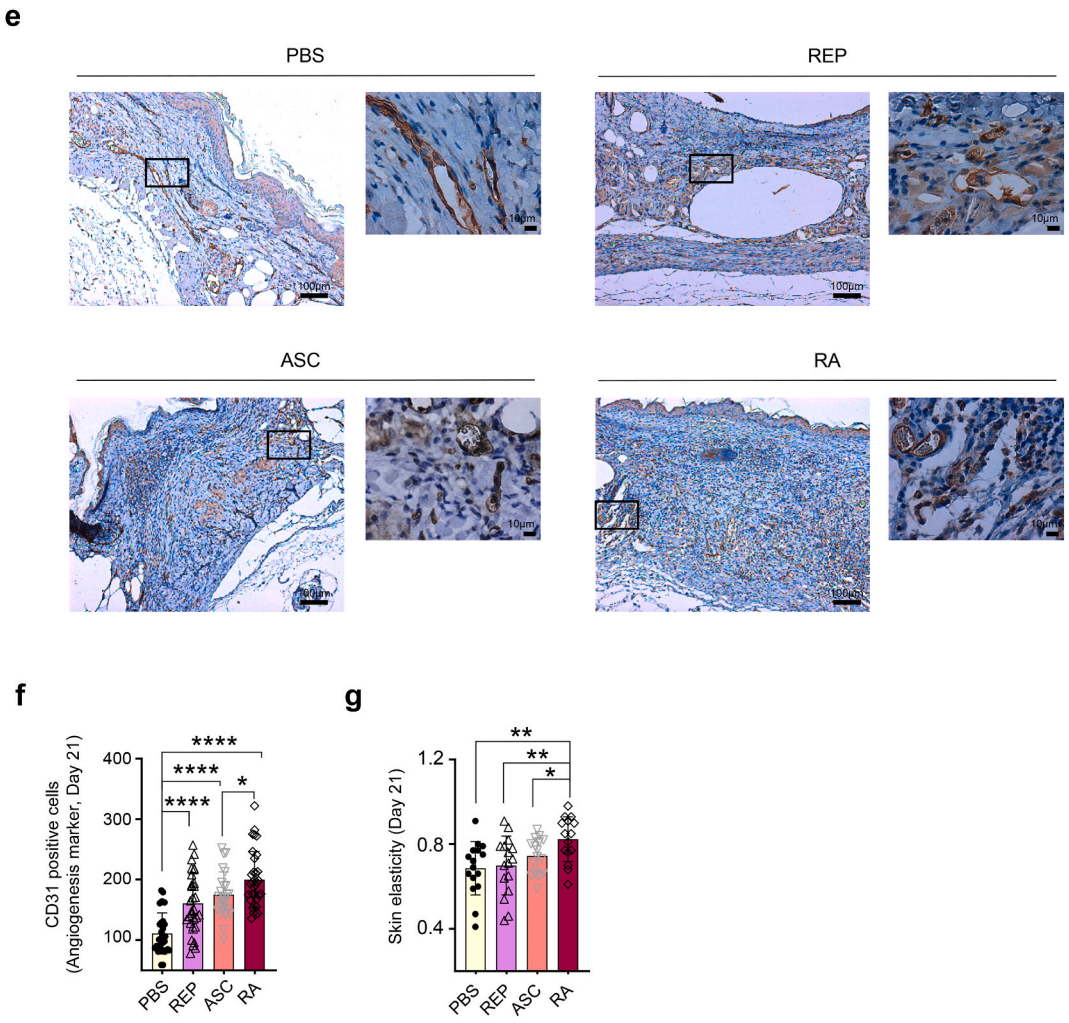

Fig. 3. (*continued*).

chronic ulceration, and, in severe cases, amputation. Although the cases of chronic nonhealing diabetic wounds is multifaceted, poor vascular networks are closely linked to the development of non-healing wounds [27]. Stem cell therapies are promising approaches for facilitating angiogenesis and healing in chronic wounds. In particular, ASCs have attracted attention owing to their paracrine effects in modulating immune responses and their ability to differentiate into vascular lineages. However, their application is limited by their poor viability in the wound microenvironment. As a result, many studies have concentrated on optimizing the viability and delivery of ASCs to wound sites to enhance their therapeutic effects [28].

In this study, we found that REPs can be used as an alternative matrix to replace damaged or lost natural ECM. Moreover, REPs were found to be effective carriers for improving the viability of transplanted ASCs. Moreover, REPs upregulated the gene expression levels of angiogenesis markers (*Cd31*, *S1*p*r1*, and *Nos3*). Previous studies have revealed the beneficial effects of the RA combination treatment on the overall wound healing process. For example, the REP-mediated ASC delivery system improves the mobilization of endogenous cells, stimulates the formation of neo-vascularization, and enhances the survival of engrafted stem cell [19]. Here, we confirmed that this system functions under conditions of impaired wound healing, such as those observed in individuals with diabetes, thereby broadening its application. We also found that Skin elasticity is significantly decreased after wound healing in diabetic mice. REPs significantly decrease skin elasticity in diabetes, causing irritation in xerotic skin [1]. Improved skin elasticity is related to improved vascular function [29]. REPs are essential for maintaining skin homeostasis during and after wound healing in patients with diabetes. Enhanced skin elasticity may occur due to improved remodeling and decreased scar formation. Therefore, REPs enhanced the functions of ASCs in skin regeneration and maintenance, suggesting that they have therapeutic potential for treating diabetic wounds in clinical settings. However, the mechanism by which REPs promote angiogenic gene expression and improve skin elasticity requires further investigation in future studies.

Author contribution statement

Conceived and designed the experiments: Young-Sam Lee and Won Bae Jeon. Performed the experiments: Seung-Hwa Woo, Joon Hyuk Choi, and Yun Jeong Mo. Analyzed and interpreted the data: Seung-Hwa Woo, Joon Hyuk Choi, Yun Jeong Mo, Yun-Il Lee, Won Bae Jeon, and Young-Sam Lee. Contributed reagents, materials, analysis tools or data: Young-Sam Lee, Yun-Il Lee, and Won Bae Jeon. Wrote the paper: Seung-Hwa Woo, Young-Sam Lee, and Won Bae Jeon.

Funding statement

This work was supported by the National Research Foundation of Korea (NRF) funded by the Ministry of Science, ICT & Future Planning (NRF-2019M3A9H1103478).

Data availability statement

No data was used for the research described in the article.

Declaration of competing interest

The authors declare the following financial interests/personal relationships which may be considered as potential competing interests: Won Bae Jeon is the founder and CEO of Excellamol Inc., and has employment and financial relationships with Excellamol Inc., including patent inventions related with REPs. All other authors have no financial conflicts of interests.

Acknowledgements

Schematic figures were adapted from “Scheme of wound healing test” by BioRender.com (2022), retrieved from https://app.biorender.com/biorender-templates. Sung-Min Kwon in the Institute of Advanced Convergence Technology (Daegu, Korea) kindly supported to use a skin elasticity measuring device.

Appendix A. Supplementary data

Supplementary data to this article can be found online at https://doi.org/10.1016/j.heliyon.2023.e20201.

References

[1] H.S. Yoon, S.H. Baik, C.H. Oh, Quantitative measurement of desquamation and skin elasticity in diabetic patients, Skin Res. Technol. 8 (4) (2002) 250–254.
[2] D.G. Greenhalgh, Wound healing and diabetes mellitus, Clin. Plast. Surg. 30 (1) (2003) 37–45.
[3] H. Seirafi, et al., Biophysical characteristics of skin in diabetes: a controlled study, J. Eur. Acad. Dermatol. Venereol. 23 (2) (2009) 146–149.
[4] B.E. Baumann L, A.S. Weiss, D. Bates, S. Humphrey, M. Silberberg, R. Daniels, Clinical relevance of elastin in the structure and function of skin, Aesthet Surg J Open Forum 3 (3) (2021 May 14) ojab019.
[5] D.S.S. Van Putte L, P. Moortgat, The effects of advanced glycation end products (AGEs) on dermal wound healing and scar formation: a systematic review, Scars Burn Heal 2 (2016 Dec 5), 2059513116676828.
[6] D.M. Bermudez, et al., Impaired biomechanical properties of diabetic skin implications in pathogenesis of diabetic wound complications, Am. J. Pathol. 178 (5) (2011) 2215–2223.
[7] D. Baltzis, I. Eleftheriadou, A. Veves, Pathogenesis and treatment of impaired wound healing in diabetes mellitus: new insights, Adv. Ther. 31 (8) (2014) 817–836.
[8] S. Ceccarelli, et al., Immunomodulatory effect of adipose-derived stem cells: the cutting edge of clinical application, Front. Cell Dev. Biol. 8 (2020) 236.
[9] J.M. Gimble, A.J. Katz, B.A. Bunnell, Adipose-derived stem cells for regenerative medicine, Circ. Res. 100 (9) (2007) 1249–1260.
[10] I.S. Park, P.S. Chung, J.C. Ahn, Adipose-derived stromal cell cluster with light therapy enhance angiogenesis and skin wound healing in mice, Biochem. Biophys. Res. Commun. 462 (3) (2015) 171–177.
[11] H.M. van Dongen Ja, B. van der Lei, H.P. Stevens, Augmentation of dermal wound healing by adipose tissue-derived stromal cells (ASC), Bioengineering 5 (4) (2018 Oct 26) 91.
[12] Z.Z. Si, et al., Adipose-derived stem cells: sources, potency, and implications for regenerative therapies, Biomed. Pharmacother. 114 (2019), 108765.
[13] Y. Kato, et al., Creation and transplantation of an adipose-derived stem cell (ASC) sheet in a diabetic wound-healing model, Jove-Journal of Visualized Experiments (126) (2017 Aug 4), 54539.
[14] A. Okamura, et al., Adipose-derived stromal/stem cells successfully attenuate the fibrosis of scleroderma mouse models, International Journal of Rheumatic Diseases 23 (2) (2020) 216–225.
[15] W. Ul Hassan, U. Greiser, W.X. Wang, Role of adipose-derived stem cells in wound healing, Wound Repair Regen. 22 (3) (2014) 313–325.
[16] C.T. Hassouneh W, A. Chilkoti, Elastin-like polypeptides as a purification tag for recombinant proteins **(Chapter 6)**(6), Curr Protoc Protein Sci (2010 Aug), 11.1-16.11.16.
[17] S.R. MacEwan, A. Chilkoti, Applications of elastin-like polypeptides in drug delivery, J. Contr. Release 190 (2014) 314–330.
[18] W.B. Jeon, B.H. Park, J. Wei, R.W. Park, Stimulation of fibroblasts and neuroblasts on a biomimetic extracellular matrix consisting of tandem repeats of the elastic VGVPG domain and RGD motif, J. Biomed. Mater. Res. 97a (2) (2011) 152–157.
[19] S.K. Choi, et al., Integrin-binding elastin-like polypeptide as an in situ gelling delivery matrix enhances the therapeutic efficacy of adipose stem cells in healing full-thickness cutaneous wounds, J. Contr. Release 237 (2016) 89–100.
[20] P. Bogdanov, et al., The db/db mouse: a useful model for the study of diabetic retinal neurodegeneration, PLoS One 9 (5) (2014 May 16), e97302.
[21] L. Dunn, et al., Murine model of wound healing, Jove-Journal of Visualized Experiments (75) (2013), e50265.

[22] P.J. Finley, R.E. Huckfeldt, K.D. Walker, L.P. Shornick, Silver dressings improve diabetic wound healing without reducing bioburden, Wounds-a Compendium of Clinical Research and Practice 25 (10) (2013) 293–301.
[23] J. Michaels, et al., db/db mice exhibit severe wound-healing impairments compared with other murine diabetic strains in a silicone-splinted excisional wound model, Wound Repair Regen. 15 (5) (2007) 665–670.
[24] A. Stachura, et al., Wound healing impairment in type 2 diabetes model of leptin-deficient mice-A mechanistic systematic review, Int. J. Mol. Sci. 23 (15) (2022) 8621.
[25] M. Wang, et al., Efficient angiogenesis-based diabetic wound healing/skin reconstruction through bioactive antibacterial adhesive ultraviolet shielding nanodressing with exosome release, ACS Nano 13 (9) (2019) 10279–10293.
[26] G. Abignano, F. Del Galdo, Quantitating skin fibrosis: innovative strategies and their clinical implications, Curr. Rheumatol. Rep. 16 (3) (2014) 404.
[27] U.A. Okonkwo, L.A. DiPietro, Diabetes and wound angiogenesis, Int. J. Mol. Sci. 18 (7) (2017) 1419.
[28] A.P. Veith, et al., Therapeutic strategies for enhancing angiogenesis in wound healing, Adv. Drug Deliv. Rev. 146 (2019) 97–125.
[29] C. Cheng, et al., Cell-assisted skin grafting: improving texture and elasticity of skin grafts through autologous cell transplantation, Plast. Reconstr. Surg. 137 (1) (2016) 58e–66e.